Ondes Gravitationnelles, Séminaire Poincaré XXII (2016) 53 – 80 Séminaire Poincaré

Detecting Gravitational Waves: Theory, Experiments and Results

David H. Shoemaker
MIT, Cambridge, MA

Catherine Nary Man - Jean-Yves Vinet
Université de Nice et Observatoire de la Côte d'Azur

Abstract. The recent historical detection of gravitational signals by LIGO ([1]) has drawn attention to the huge amount of work which has been needed for obtaining, after more than thirty years of technological efforts, this breaking result. Moreover, enhancement of the sensitivity of the existing detectors as well as plans for future instruments is likely to attract new scientists, so that it seems useful to recall the background of this field of research. Obviously we will present the state-of-the-art in operating detectors. It is also likely, after the success of LISA Pathfinder ([2]) that spaceborne detectors will trigger a larger interest, and that the very long wavelength band will be explored in the coming decades.

1 Action of gravitational waves on light

The idea of using light for testing space's curvature is as old as General Relativity. Deflexion of light rays by the gravitational field of the sun was the first direct observational test of a general relativistic geometric effect. This led several scientists to propose to detect gravitational waves through dynamic anomalies in the propagation of light ([3]). The topology of a Michelson interferometer was soon proposed ([4]) for this kind of experiment. Consider now a weak gravitational field described by the metric tensor

$$g_{\mu\nu}(t,\vec{x}) \;\equiv\; \eta_{\mu\nu} \;+\; h_{\mu\nu}(t,\vec{x}) \tag{1}$$

where $(ct,\vec{x})$ (c : speed of light) are the flat spacetime ordinary coordinates, $\eta_{\mu\nu} \equiv \mathrm{diag}(1,-1,-1,-1)$ the Minkowski tensor, and $h_{\mu,\nu}(t,\vec{x})$ a gravitational wave of weak amplitude, so that the coming calculations will be at first order in h. The invariant space-time element ds^2 is given in arbitrary coordinates $x^\mu, (\mu = 0,1,2,3)$ by

$$ds^2 = g_{\mu\nu}dx^\mu dx^\nu. \tag{2}$$

It exists a special gauge choice (TT gauge) and a coordinate system, for a given source, such that the tensor $h_{\mu\nu}$ is reduced to 2 independent components. If $\vec{w}$ is unit vector pointing to the source, one can find two unit vectors $\vec{a}$ and $\vec{b}$ orthogonal and spending the transverse plane : $\vec{a}.\vec{b} = \vec{a}.\vec{w} = \vec{w}.\vec{b} = 0$. Then we have simply

$$h_{0i} = 0 \ (i = 1,2,3), \quad h_{ij} = h'_+(a_ia_j - b_ib_j) + h'_\times(a_ib_j + a_jb_i). \tag{3}$$

If now we consider the two vectors $\vec{\theta}$,$\vec{\phi}$ naturally related to the observation direction:

$$\vec{\theta} \equiv \frac{\partial\vec{w}}{\partial\theta} \quad \vec{\phi} \equiv \frac{1}{\sin\theta}\frac{\partial\vec{w}}{\partial\phi}.$$

We get

$$h_{ij} = h_+(\theta_i\theta_j - \phi_i\phi_j) + h_\times(\theta_i\phi_j + \theta_j\phi_i) \tag{4}$$

where the new components $(h_+, h_\times)$ are related to the intrinsic ones $(h'_+, h'_\times)$ by a rotation of angle 2α, which nothing but the angle between $\vec{\theta}$ and $\vec{a}$ (due to the spin 2 nature of the field). Consider now a trip in a vacuum along a direction defined by the unit vector $\vec{n}$: We get for the ds^2 :

$$0 \;=\; c^2dt^2 - dl^2 \;+\; h_+(t - \vec{w}.\vec{x}/c)[(\vec{\theta}.\vec{n})^2 - (\vec{\phi}.\vec{n})^2] + 2h_\times(t - \vec{w}.\vec{x}/c)(\vec{\theta}.\vec{n})(\vec{\phi}.\vec{n}) \tag{5}$$

so that

$$c^2dt^2 = [1 + H(t - \vec{w}.\vec{x}/c)]dl^2 \tag{6}$$

with

$$H(t) \equiv h_+(t)[(\vec{\theta}.\vec{n})^2 - (\vec{\phi}.\vec{n})^2] + 2h_\times(t - \vec{w}.\vec{x}/c)(\vec{\theta}.\vec{n})(\vec{\phi}.\vec{n})$$

and, at first order in H :

$$dl \;=\; cdt \;-\; \frac{c}{2}\,H(t - \vec{w}.\vec{x}/c)\,dt. \tag{7}$$

We assume a trip from A to B beginning at $t = t_0$ ending at $t = t_1$, $(\vec{x}(t) = \vec{x}_A + c(t - t_0)\vec{n})$. At the lowest order, we have obviously $t_0 = t_1 - L/c$, so that

$$L \;=\; c(t_1 - t_0) + \frac{c}{2}\int_{t_1 - L/c}^{t_1} H[(1 - \vec{w}.\vec{n})t + t_0\vec{w}.\vec{n} - \vec{w}.\vec{x}_A/c]\,dt. \tag{8}$$

In this expression, t_0 appears now as the retarded time, i.e. the time at which was emitted the photon received at t_1. Replacing now t_1 by t (current tome) and t_0 by t_R (retarded time) we get

$$t_R \;=\; t \;-\; \frac{L}{c} \;+\; \frac{1}{2}\int_{t - L/c}^{t} H[(1 - \vec{w}.\vec{n})t' + t\vec{w}.\vec{n}/c \,-\, \vec{w}.\vec{x}_B/c]\,dt'. \tag{9}$$

Let us assume now that the wave amplitude H admits a Fourier transform (which certainly is the case for a transient signal):

$$H(t) \;=\; \int_{\mathrm{R}} \tilde{H}(\Omega)\, e^{-i\Omega t} d\Omega$$

the result is

$$t_R \;=\; t - \frac{L}{c} + \frac{1}{2}\int_{\mathrm{R}} \tilde{H}(\Omega)\, e^{-i\Omega[t - L/c - \vec{w}.\vec{r}_A/c]}\, \frac{1 - e^{-i\Omega L(1 - \vec{w}.\vec{n})/c}}{i\Omega(1 - \vec{w}.\vec{n})}. \tag{10}$$

1.1 Antennas short compared to the gravitational wavelength

If the propagation range is much shorter than the gravitational wavelength, which is the case for ground based interferometers, delays of order L/c in the signal can be neglected, owing to the scanned frequency range (from a few Hz to a few hundred Hz). The retarded time for a round trip propagation is thus simply

$$t_R = t - \frac{2L}{c} + \frac{L}{c}H(t).$$

1.2 Antennas long compared to the gravitational wavelength

In spaceborne detectors, the laser links are several Mkm long, so that the preceding approximation cannot be used any more. The detection process, as will be explained later, is based on the beat note at B between the coming light wave emitted in A and a local oscillator. We therefore are interested in the phase modulation. If the frequency of the laser A is ν_A, the phase detected at B is, after equation (10) :

$$\phi_B(t) \;=\; \phi_A(t) - \; 2\pi\nu_A L/c$$
$$+ \; \frac{\pi\nu_A}{c} \int_{\mathrm{R}} \tilde{H}(\Omega)\, e^{-i\Omega[t-L/c-\vec{w}.\vec{r}_A/c]}\, \frac{1-e^{-i\Omega L(1-\vec{w}.\vec{n})/c}}{i\Omega(1-\vec{w}.\vec{n}))} \tag{11}$$

We see that the frequency detected at B, assuming ν_A a constant, is modulated, according to

$$\frac{\delta nu}{\nu_A}(t) \;\equiv\; \frac{1}{2\pi\nu_A}\frac{d\phi_B}{dt}$$

or

$$\frac{\delta\nu}{\nu_A}(t) \;=\; \frac{1}{2}\frac{H(t-\vec{w}.\vec{r}_B/c) - H(t-\vec{w}.\vec{r}_A/c - L/c)}{1-\vec{w}.\vec{n}}. \tag{12}$$

The effect may thus be viewed as a dynamical Doppler shift.

2 Michelson Interferometers

A preliminary remark could be useful for what follows. Consider any transducer system, i.e. a device transmitting light and having its output modulated by an external perturbation $x(t)$. The incoming power (laser) is P_L, the ouput power is $P(t)$. In absence of perturbation ($x = 0$), the output power is $P = \alpha P_L$, where α is the system's transmittance. The optical detection, in that situation, generates at least a quantum noise of linear spectral density (SD) :

$$S^{1/2}_{\mathrm{out,x=0}}(f) \;=\; \sqrt{2\alpha P_L h_P \nu}$$

(where ν is the light frequency, and h_P Planck's constant). If the perturbation acts, the output is now (linear regime, corresponding to a very small $x(t)$):

$$P(t) \;=\; [\alpha + \beta x(t)]\, P_L \tag{13}$$

where β is a scale factor. This means that the SD of signal is related to the SD of the perturbation $S_x^{1/2}(f)$, by

$$S^{1/2}_{\mathrm{out,x}}(f) \;=\; \beta P_L S_x^{1/2}(f)$$

so that eventually, the signal to noise ratio is

$$SNR(f) \;\equiv\; \frac{S^{1/2}_{\mathrm{out,x}}(f)}{S^{1/2}_{\mathrm{out,x=0}}(f)} \;=\; \frac{\beta\sqrt{P_L}}{\sqrt{\alpha h_P \nu}}\, S_x^{1/2}(f). \tag{14}$$

Besides the obvious remark that the scaling factor β should be as large as possible, we note that for this limitation to sensitivity it is recommended to have as large as possible a laser power P_L, and as small as possible a transmittance α. This explains

why in developing laser interferometers for detecting weak gravitational waves, we look for powerful lasers, or means for increasing the power, and why we try to obtain such a good constrast that the output fringe is as 'dark' as possible. We note that there is a maximum of laser power that is ideal for measurement at a given frequency. The transfer of momentum from the light to the optics of the Michelson interferometer grows with light power, causing a motion of the optics with a $1/(mf^2)$ characteristic. Thus, we have a 'Heisenberg Microscope' for which one can, given an optic mass m and a desired measurement frequency f_d, choose an optimum power P_d for the laser.

2.1 Simple Michelson

The basic configuration proposed more than 50 years ago more independently by several physicists, (see for instance R. Weiss[9]), is the Michelson setup. The Michelson topology is contained in a plane which can be defined by two orthogonal unit vectors $\vec{n}_N$ and $\vec{n}_W$ corresponding to the light propagation in the North and West (generic names) arms respectively. We consider here a system with optics free of wavefront errors, acting as test masses free to respond to a passing gravitational wave, an ideal laser, and in the shot-noise limited regime (low laser power and large optic masses). After formula (8), we get two versions (N,W) of the light modulation:

$$H_N(t) = h_+(\cos^2\theta\cos^2\phi - \sin^2\phi) \; - \; h_\times \cos\theta \sin 2\phi \tag{15}$$

$$H_W(t) = h_+(\cos^2\theta\sin^2\phi - \cos^2\phi) \; + \; h_\times \cos\theta \sin 2\phi \tag{16}$$

we see that there is in general a differential effect in the two arms, and morover, if the incidence angle is normal with respect to the plane (NW)(i.e. $\theta = 0$), there exist angles ϕ such that $H_N = -H_W = h_+$ (for $\phi = 0$, and $H_N = -H_W = -h_\times$, for $\phi = \pi/4$). The perturbation $x(t)$ introduced in eq.(13) may be viewed here as a length change in the two arms, in opposite phase ($\pm x(t)/2$) (see Fig.(1). Let us call a and b the lengths at rest of the two arms, r_1 and r_2 the reflection coefficients of mirrors M_1 and M_2, and P_L the input power. The transmission and reflection coefficients of the splitter are (t_s, r_s). The laser frequency is $\nu \equiv c/\lambda$. It is easily found that the output power P on the B port of the setup is given by

$$P \; = \; P_L r_s^2 t_s^2 \left[r_1^2 + r_2^2 + 2r_1 r_2 \cos\alpha - 4r_1 r_2 k x(t) \sin\alpha\right] \tag{17}$$

where $k \equiv 2\pi/\lambda$ and $\alpha \equiv 2k(b-a)$. The signal to noise ratio can be obtained as (we assume $rs^2 \simeq ts^2 \simeq 1/2$)

$$\rho(f) \; = \; 2r_1^2 r_2^2 \frac{P_L}{h_P \nu} k^2 S_x(f) \, \frac{\sin^2\alpha}{r_1^2 + r_2^2 + 2r_1 r_2 \cos\alpha} \tag{18}$$

where $S_x(f)$ is the spectral density of x seen as a stochastic process. There is an optimum in the SNR (see [6]) for $\cos\alpha = -r_1/r_2$ (assuming $r_1 < r2$). If both r_1, r_2 are close to 1, we find

$$\rho_{opt}(f) \; = \; \frac{2P_L}{h_P \nu} k^2 S_x(f). \tag{19}$$

Taking now $a = b = L$ and $x = h \times L$, a SNR of 1 gives the spectral sensitivity of the setup in terms of the gravitational wave amplitude h:

$$S_h^{1/2}(f) \; = \; \frac{\lambda}{4\pi L} \sqrt{\frac{2h_P\nu}{P_L}}. \tag{20}$$

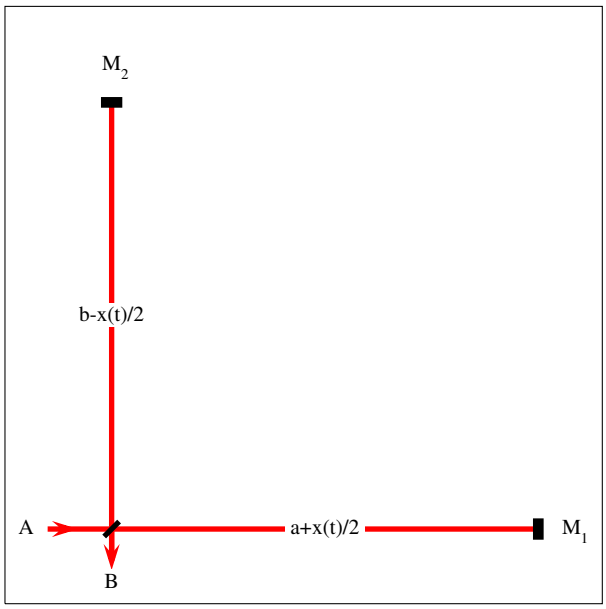

Figure 1: Basic Michelson interferometer

With 3 km arm length and a YAG laser ($\lambda \simeq 1.064\mu$m), of power 100W, this gives a sensitivity of the order of 10^{-21} Hz$^{-1/2}$, which is at least two orders of magnitude too high for a realistic detection rate. This is why several ideas have been proposed and developed for increasing L and P_L in the preceding basic formula. Remark that the power reflected by the Michelson is

$$P_{\rm ref} \;=\; P_L\,\left[t_s^4 r_1^2 + r_s^4 r_2^2 \;-\; 2 r_s^2 t_s^2 \cos\alpha\right]$$

so that with the optimal tuning and ($r_2 \equiv r + \delta r/2 > r_1 \equiv r - \delta r/2$), this is

$$P_{\rm ref}/P_L \;=\; r^2(t_s^2 + r_s^2) + r\delta r(r_s^4 - t_s^4) \tag{21}$$

considering that the splitter is well balanced ($r_s^2 \sim t_s^2$) and introducing the total losses p_s of the splitter and p_M of the mirrors, we get, neglecting second order terms

$$P_{\rm ref}/P_L \;\simeq\; 1 - p_M - p_s \tag{22}$$

showing that the global reflectance is near unity when the Michelson is tuned at a dark fringe.

2.2 Fabry-Perot cavities

A Fabry-Perot cavity involves two mirrrors facing each other and separated by a length L (see Fig.(2). We assume mirror M_2 highly reflective, and mirror M_1 partially reflective. It is classically shown that such a simple setup exhibits resonance peaks in the intracavity power ($|E|^2$) for special frequencies separated by the free spectral range (FSR) The FSR is given by

$$\Delta\nu_{\rm FSR} \;=\; \frac{c}{2L}.$$

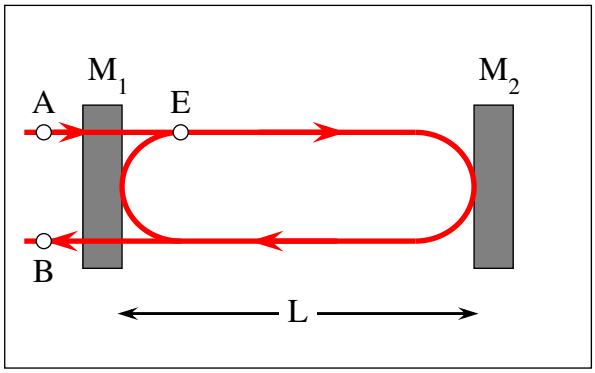

Figure 2: A Fabry-Perot cavity and resonant arms

If we denote r_1, r_2 the reflection coefficients of the two mirrors, we can define the finesse by (see Fig.(2 for notation) :

$$\mathcal{F} \;=\; \frac{\pi\sqrt{r_1 r_2}}{1 - r_1 r_2}. \tag{23}$$

If a resonance occurs at frequency ν_0, the width of the corresponding resonant peak (i.e. twice the detuning with respect to ν_0 such that the intracavity power falls to half its maximum value) is given by

$$\delta\nu_{\rm FWHM} \;=\; \frac{\Delta\nu_{\rm FSR}}{\mathcal{F}}. \tag{24}$$

Moreover, if p denotes the total losses of the two mirrors (i.e. the fraction of light power which is lost by absorption, scattering, etc...on the two mirrors), we can construct the parameter $\sigma \equiv p\mathcal{F}/\pi$, called the coupling coefficient (see [6]), which is extremely relevant for estimating the properties of Fabry-Perot cavities. We can denote by $f \equiv (\nu - \nu_0)/\delta\nu_{\rm FWHM}$ the reduced detuning. Provided that $|\nu - \nu_0| \ll \Delta\nu_{\rm FSR}$, or equivalently $f \ll \mathcal{F}$, we get (assuming $\mathcal{F} \gg 1$) :

$$|E/A|^2(f) \;=\; \frac{2\mathcal{F}}{\pi}\,\frac{1-\sigma/2}{1+4f^2}$$

while the global reflectance of the cavity is

$$\mathcal{R}(f) \;=\; -\,\frac{1-\sigma+2if}{1-2if} \tag{25}$$

so that the reflectance at resonance is $\mathcal{R}_(0) = -(1-\sigma)$. We see that if the cavity is a subsystem used in reflection, it is essential to have such low losses that $\sigma \ll 1$. In that case, the peak resonance value for the stored power is simply $\mathcal{S} \equiv |E/A|^2(0) \;=\; \frac{2\mathcal{F}}{\pi}$. It can also be shown that a small change δL in the length of the cavity produces a change in the reflected phase

$$\delta\Phi \;=\; \mathcal{S} \;\times\; \frac{4\pi\delta L}{\lambda} \;=\; \delta\Phi \;=\; \mathcal{S} \;\times\; \delta\Phi_0$$

where $\delta\Phi_0$ would be the phase change is absence of an input mirror. In other word, we have an amplification factor $\mathcal{S}$ in phase with respect to a single round trip, and the same factor for the stored power. These considerations led to the use of Fabry-Perot cavities for increasing the power reaching the splitter, and to have effective lengths of the arms much larger than the geometrical ones.

2.3 Power Recycling

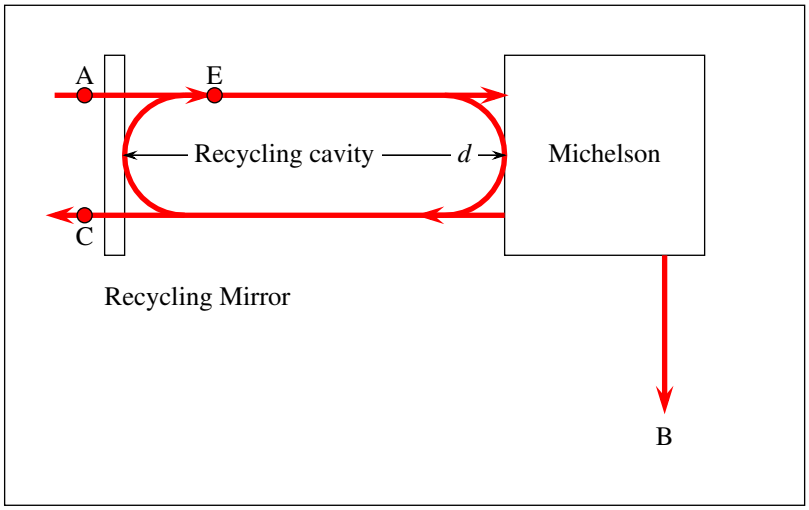

Figure 3: Recycling setup.

If we use the preceding result (25), we see that the reflectance at resonance of one arm is $r_{\text{fp}} = -(1-\sigma)$ where $\sigma \ll 1$. If on the other hand we apply eq.21, we conclude that the global reflectance of the Michelson with resonant arms is :

$$r_M ic \;=\; \sqrt{1-p_s-2\sigma} \;\simeq\; 1-\sigma-p_s/2.$$

The Michelson behaves thus as a virtual mirror of high reflectance. This suggested the idea of adding a recycling mirror, i.e. a mirror placed in front of the Michelson (see Fig.3) and building a resonant cavity able to increase the power reaching the splitter, and enhancing this way the signal to quantum noise ratio. It can also be seen as an impedence matching of the incoming laser light to the (slightly) lossy Michelson 'mirror', and was exploited in the microwave domain in the 1940's. The idea was brought to use in the domain of lasers independently by R. Drever ([5]) and R. Schilling, and experimentally demonstrated by A. Brillet.

2.4 External noises

The small change in optical path due to a gravitational wave competes with a lot of perturbations causing a noise which, unless significant measures are taken, are far larger than what one tries to detect. In particular, if the light beams were propagating in the free atmosphere, the index fluctuations caused by pressure fluctuations (sound noise, wind,...) would generate a forbidding noise. All optical paths are

therefore enclosed in a ultra-high vacuum system. In Virgo for instance, there are two vacuum pipes enclosing the Fabry-Perot cavities, with residual pressure better than 10^{-9} mbar. This for a 2.3 Ha internal surface (to be outgassed).
A second external influence is the seismic noise. If the mirrors were directly related to the ground, its vibrations due to natural or human activity would hide the signal. The spectral density of displacement is currently around $10^{-7}\,\mathrm{m} \times \mathrm{Hz}^{-1/2}$. One approach to seismic isolation is for the mirrors to be suspended from a series of filters (see Fig.4) cascading their individual transfer functions of a $1/f^2$ characteristic. The global transfer function is of the order of 10^{-18} at a frequency of 100 Hz.

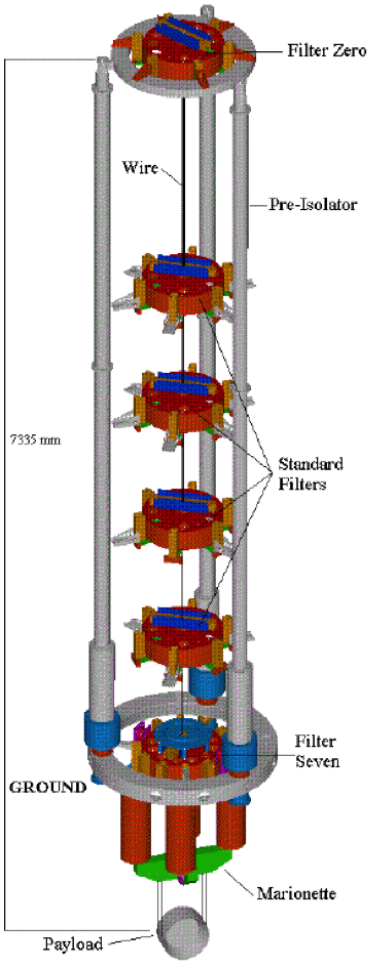

Figure 4: A Virgo superattenuator.

2.5 Internal noises

Several internal noises are due to thermal excitation of the optics (or test masses). Being operated at room temperature, all mechanical resonators (the suspended test masses, the bulk of the mirrors, the coatings of the mirrors...) receive energy $k_B T$ per degree of freedom. Again, the result is a prohibiting noise. It is however possible to concentrate the noise in extremely narrow frequency intervals around resoanance, by

using high quality factors ("Q") in the various systems. For instance, the suspended mirrors have resonances frequencies much lower than 1 Hz, so that the resulting thermal noise is highly reduced in the detection band.
The Brownian motion inside the bulk material of the mirrors can be reduced by using low mechanical loss fused silica ($Q \sim 10^7$), and by using optical beams of large transverse size (see [8]).

3 Advanced Virgo

3.1 From Virgo to Advanced Virgo

The initial Virgo project was a joint initiative of the C.N.R.S. (France) and I.N.F.N. (Italy). Dutch teams from Nikhef, from the Polish and Hungarian Academies of Science joined later the project. The construction of the infrastructure of Virgo began in year 1999, and the target sensitivity was met in 2011. This was the first phase, showing that an impressing sensitivity was possible with the 1990's technology (see Fig.5). It was nevertheless foreseen from the beginning that such a sensitivity would probably be too poor for significant observations from an astrophysical point of view. After "Initial Virgo", the funding agencies allowed the next phase, called "Advanced

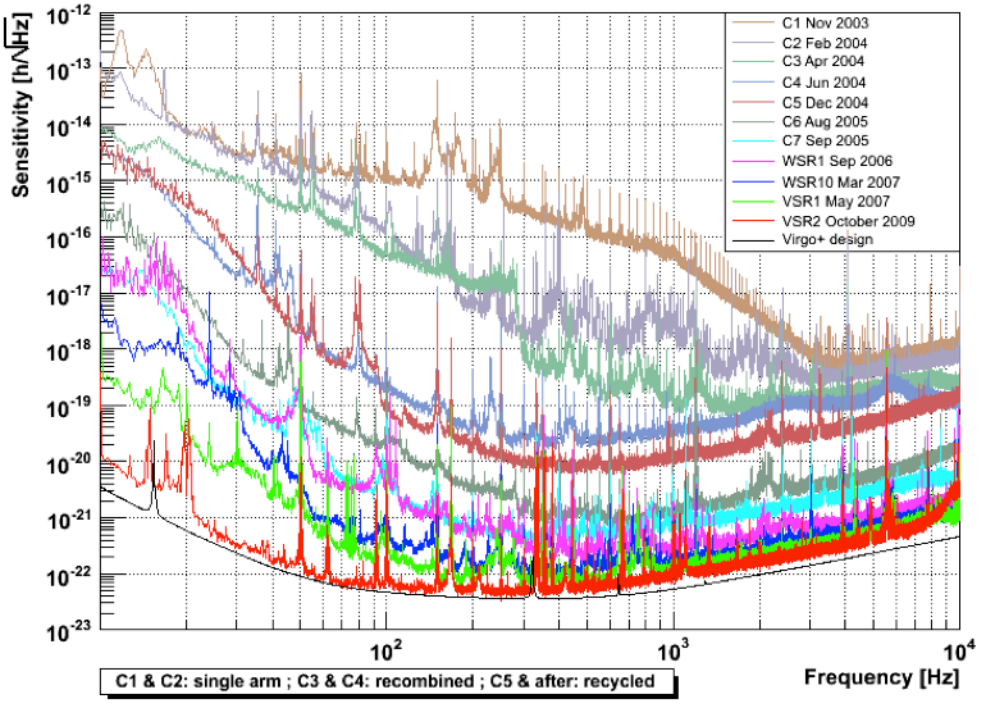

Figure 5: Evolution of Virgo's sensitivity.

Virgo", aiming to win one order of magnitude in the sensitivity. The infrastructure stays unchanged (see Fig.6), but many subsystems have been improved.

Figure 6: Aerial view of the Virgo site at Cascina (near Pisa, Italy).

3.2 Some parameters

In the initial configuration, mirror technology indicated specific ratios of power recycling and arm finesses. The recycling gain was about 50, and the finesses approximately 160. In the"advanced" version, the philosophy is different. Knowing that high powers are expected to circulate in the instrument, and that the recycling cavity is only marginally stable, thus sensitive to non-linear optical effects, it was decided to have a moderate recycling gain of ~ 37.5. On the other hand, the quality of the mirror surfaces having increased by a large amount, a high finesse is allowed for the arm cavities (~ 450).

3.3 Mirrors

Obtaining high quality mirrors has been a key issue from the beginning of the LIGO-Virgo adventure. Multilayer treatment of large (35 cm diameter) objects being a very special task, a dedicated facility has been built jointly by CNRS (F) and INFN (I) near Lyon (F) (see 7). It now produces mirrors and splitters for the LIGO-Virgo Collaborations with absorption of 0.2 ppm and scattering losses of the order of tens of ppm.

3.4 Signal Recycling

A significant improvement to be implemented in Advanced Virgo is the "Signal recycling" setup, proposed years ago by B. Meers ([7]). By adding a resonant cavity on the output port of the Michelson (see Fig.8), it is possible to change the shape of the sensitivity curve in order, for instance to concentrate the sensitivity in a frequency range optimizing for both instrumental limitations and astrophysical source characteristics. Different scenarios are foreseen for Virgo. Starting from a simple power

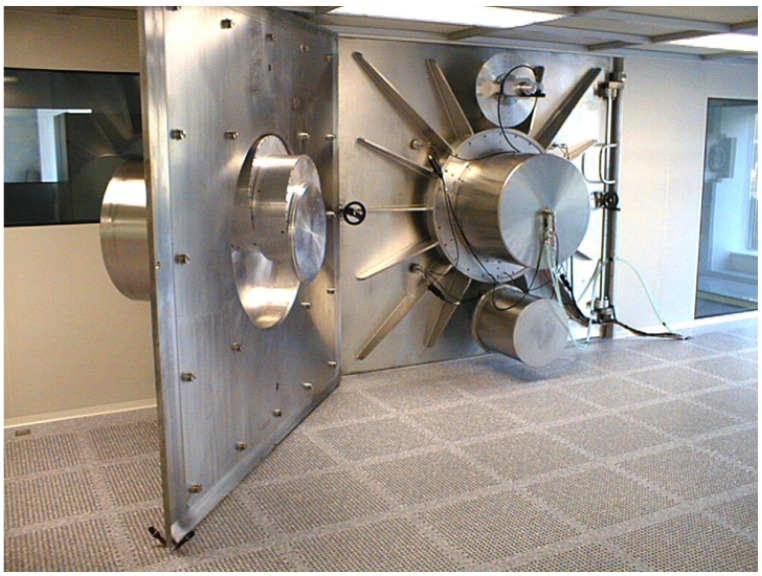

Figure 7: Large Coater Facility at the Laboratoire des Matériaux Avancés (Institut de Physique Nucléaire, Lyon, France).

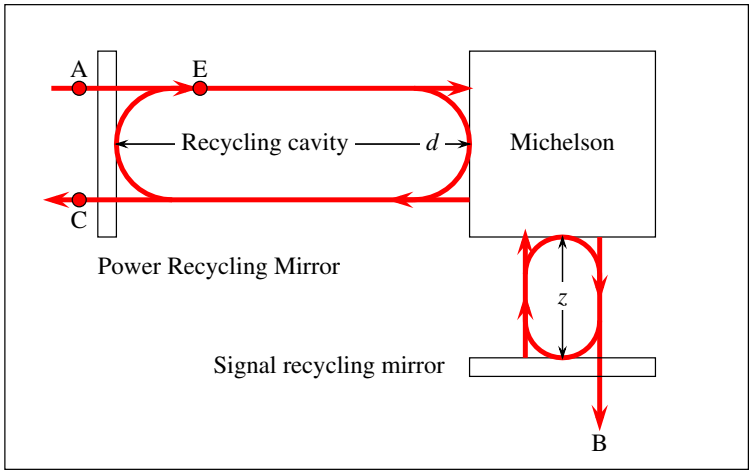

Figure 8: Signal recycling cavity.

recycled interferometer, and going towards different strategies of signal recycling (see Fig.9).

4 Advanced LIGO

4.1 LIGO

The LIGO Project had its inception in early work by Rai Weiss of MIT in the late 1960's and early '70s([9]). As noted above, he was one of a number of researchers around the world who more or less independently conceived of the notion of using laser interferometry as a way of sensing the path length change due to a passing gravitational wave. Weiss' unique and enduring contribution was to work through

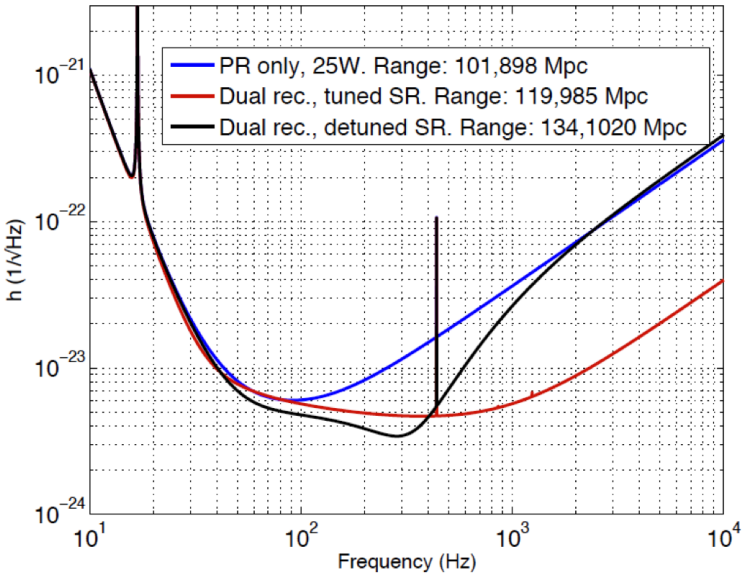

Figure 9: Planned evolution for the Advanced Virgo sensitivity (Range indicated for binary neutrons star coalescences).

the limitations to sensitivity – both fundamental and practical, and to establish a scale of an instrument that could, with the astrophysical understanding of the time, plausibly make detections. Kip Thorne of Caltech had already put significant thought into both potential sources and the basic physics of detection when he and Weiss met in the early 1970's and resolved to try to realize instruments in the US to start this new field of gravitational wave astronomy.

Several physicists in the US National Science Foundation (NSF) became strong advocates for this endeavor, notably Rich Isaacson and Marcel Bardon, and funding for small-scale proof-of-principle experiments was made available. An industrial study was performed in parallel, investigating the practicalities of making km-scale interferometers and helping to establish a cost and schedule baseline. By 1989, a proposal had been submitted for LIGO: two 4km-arm-length instruments to be built separated by thousands of km, and with the capability of supporting both initial instruments with the technology of the time, but also with the foresight to include flexibility for later, more sensitive instruments.

Scientists and engineers worked together to both understand and reduce the so-called 'fundamental' noise sources of photon shot noise and thermal noise through more elaborate interferometer topologies, fringe interrogation systems, and laser development, as well as better understanding of the fluctuation-dissipation theorem and its guidance to choose low-mechanical-loss materials and to engineer designs which made the most of the materials available. New expertise developed in the multi-disciplinary domain of 'commissioning' which required an understanding of all aspects of the instrument performance, and a very significant and difficult transition was made from small to Big Science. With this transition came both the need for and development of scientific and engineering managers who could coordinate the activities of hundreds of scientists and engineers, and spend hundreds of millions of dollars of taxpayer's money responsibly and transparently.

Continued research and development led to a plausibly-sensitive design, and engineering and civil construction led to the completion of the Livingston, Louisiana (shown in Fig.10) and Hanford, Washington LIGO Observatories by roughly the year 2000. The instruments were installed, and slowly but surely brought to their full sensitivity by 2005. A series of observing runs, also with Virgo, followed.

Figure 10: LIGO Observatory in Livingston, Louisiana. The Hanford, Washington Observatory is very similar. *Credit: LIGO/MIT/Caltech.*

In parallel with the development of the instruments, a growing number of scientists were working on the challenges of interpreting the data from the instruments. This required astrophysicists to search out and characterize the waveforms from potential gravitational-wave signal sources, and scientists who worked on understanding the imperfections in the data; it is far from white, stationary, Gaussian noise. It also required expertise in programming and data management due to the significant computing demands.

The conjunction of these instrument scientists, engineers, highly specialized technicians, astrophysicists, and signal analysis experts joined together to form the LIGO Scientific Collaboration (LSC) in the late 1990's. The synergy of these skills delivered results in the form of a series of astrophysical upper limits and interesting non-detections in the time from 2005-2015. The NSF had placed a requirement on LIGO to observe for one full integrated year, at design sensitivity, and this was achieved in 2008. That enabled the official start of Advanced LIGO, discussed in the next section.

4.2 Advanced LIGO

As noted above, the design of the LIGO Observatories foresaw the need for further generations of instruments to move from plausible to probable detection sensitivity. World-wide research and development continued through the 1990's while LIGO and Virgo were being built, coordinated by the then-new LSC, and by 1999 a White paper was written by Gustafson, Shoemaker, Strain, and Weiss[17] which collected the progress in instrument science together into a coherent vision for the second

generation of LIGO instrument.

4.2.1 Philosophy

The program to develop a successful second-generation instrument was tightly focused around a reference design for Advanced LIGO, which was planned to be a quantum-limited interferometer with a very significant increase in sensitivity over initial LIGO. A smaller but vital continuing research plan for future detector development was also laid out. A companion conceptual plan for the schedule and projected cost for the full-scale implementation of the baseline had been developed by the LIGO Laboratory in close coordination with the LSC research plan.

The guiding considerations in designing the research and development program were:

- broadening the detectors sensitive band by reducing the limiting noise terms,
- the reduction of the noise in the spectral region of maximum sensitivity around 100 Hz,
- the assessment of the technical maturity and feasibility of the improvement,
- the increase in detection range of anticipated astrophysical sources,
- the need to maintain both a near term development program and a long range basic research effort to exploit the capabilities of the LIGO facilities.

The LSC chose a very compact characterization for the Advanced LIGO sensitivity goal: a factor of 10 in reach for neutron-star binaries. This increase of 1000 in the number of candidates, with the estimates of rates at that time, made detection of an NS-NS binary probable in a one-year observing campaign. In fact, due to the improved low-frequency performance, it increased the sensitivity to more massive binaries by a far larger figure.

After exploration of various engineering approaches, it was also concluded that a one-time complete replacement of the detector was needed. This was due to the marginally effective seismic isolation system for initial LIGO in the gravitational-wave band, and its poor damping below the gravitational-wave band. Replacing the seismic isolation necessitated the removal of all of the rest of the instrument, and so the opportunity was taken to design a completely new instrument.

Other lessons learned from initial LIGO related to the optical design; initial LIGO used a marginally stable power recycling optical cavity, meaning that very small deviations from alignment or mirror figure would easily couple light power out of the desired TEM_{00} fundamental Gaussian mode. This proved to be challenging for both the alignment control and the tolerance to deformations in the optics due to absorbed light power. Thus, for both power recycling and the to-be-added signal recycling cavities, focusing elements were introduced to improve the stability of the optical modes.

LIGO also had difficulty in initial LIGO to take advantage of the second interferometer, installed with parallel light paths to the first interferometer but with 2km rather than 4km arms, due to both practical issues with the realization of a 'folded' interferometer and also just due to limitations in the staffing to bring two instruments rather than one to design sensitivity. More importantly, the maturing

data analysis effort and the promise of multi-messenger astronomy showed the enormous value of putting a detector out of the effective plane established by LIGO and Virgo – encouraging an additional site to the South. Thus a search was started for partners who could provide an infrastructure to house the 3rd interferometer.

Perhaps the most important lesson learned, however, was the importance of quality control. While it sounds mundane, the complexity of the instrument was such that having assembled initial LIGO without full testing to performance requirements of each assembly separately in advance led to a very long and indirect commissioning sequence. A great deal of time was lost fixing – or even redesigning, manufacturing, and replacing – parts which could not function as installed. For Advanced LIGO, we resolved to take the time 'up front' to make instruments which had a much higher probability to function when first assembled.

4.2.2 Key Technologies

To realize the increase in sensitivity, the 'fundamental' noise sources – thermal noise, and quantum limits to the sensing – had to be addressed. For the former, a solution proposed by the Glasgow University group was adopted. The concept for management of thermal noise in the interferometric gravitational-wave detectors is, as mentioned above, to select materials of low internal mechanical loss. (This can be complemented by lowering the temperature to directly reduce $k_{\rm B}$T as is planned for KAGRA, the Japanese detector, but LIGO and Virgo currently plan room-temperature operation.) The integral under the curve of physical motion in a degree-of-freedom due to thermal energy remains $k_{\rm B}$T, but per the fluctuation-dissipation theorem the bulk of the motion is gathered under the peak of the mechanical resoance of the degree-of-freedom, and the amplitude above and below in frequency is reduced.

The Glasgow University group had created a monolithic assembly (see Fig.11) of a fused-silica test mass bonded as one with thin fused-silica fibers; this pendulum suspension technique was already familiar from the first generation of instruments, but for first-generation detectors, metal wires which are relatively mechanically lossy had been used. Measurements of the Q of fused-silica assemblies were very promising and the modeling of real materials with additional loss mechanisms (thermoelasticity in particular) showed that a suspension system could realize the reduction by a factor of 10 for neutron star binaries, and also deliver better low-frequency performance as well. A consortium in the UK made the contribution of the suspensions for Advanced LIGO.

A second key technology is in interferometer topologies. After an early insight by Brian Meers of Glasgow showed the advantages of adding a signal recycling mirror, a number of laboratories worked to demonstrate the feasibility of using the approach, and it was appreciated that it not only allowed changes to the sensitivity curve of the instrument, but had two very interesting additional features. First, it allowed the management of power distribution in the interferometer, and as higher circulating power was anticipated to reduce the high frequency noise, this was very useful to bring the thermal lensing due to optical absorption under control. This allowed Advanced LIGO to adopt a design employing as much as 180 W of input laser light, and the Hannover Max Planck Albert Einstein Institute offered to supply the laser for the instruments.

In addition, signal recycling has the interesting virtue of coupling the quantum

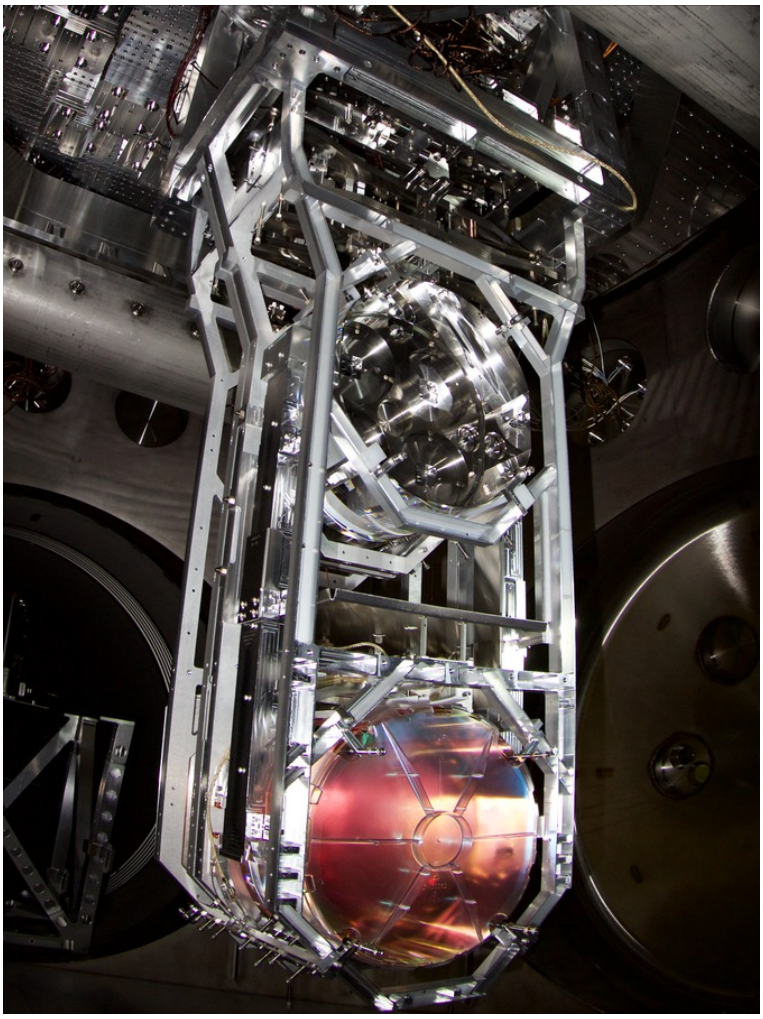

Figure 11: Advanced LIGO Suspension system. The test mass, which also serves as the Michelson end mirror, is at the bottom; a protective cover is in place. *Credit: LIGO/MIT/Caltech.*

power fluctuations in the light due to the nominally Poisson statistics of the photons with the phase fluctuations – the momentum transferred to the test masses moves them, which shifts the phase of the light. Thus, there is pondermotive squeezing in the interferometer, which influences the sensitivity, adds some dynamics to the servo control system, and can be both a virtue and a complication in bringing the instrument to high sensitivity.

As mentioned above, an additional change in the optical configuration was the addition of focusing elements in the recycling cavities, which relaxed mirror figure requirements, alignment requirements, and facilitated the ability to work with a range of input laser powers.

The third key technology in Advanced LIGO is the seismic isolation system. After a great deal of analysis and prototyping, Advanced LIGO chose a system of high-gain servocontrolled platforms for seismic isolation; early efforts at JILA by Joe Giaime and colleagues, and then at Stanford led by Brian Lantz provided the proofs-of-principle and then much of the engineering. In this approach, motion sensors (displacement, velocity, and acceleration sensors are all employed) sense motion

of the platform to be controlled. The sensors develop signals which are amplified and distributed to actuators to counter the sensed motion. In principle, the motion of the platform can be brought to the thermal noise of the sensor test mass. In practice, there are a number of complexities. An agreeably fundamental issue, and one of interest to our friend Einstein, is the equivalence principle – the horizontal accelerometers cannot distinguish between a horizontal acceleration and a tilt (which couples the nominally horizontal sensing axis to the vertical gravitational acceleration). Many more prosaic issues are also present, having to do with resonances in the mechanical structures limiting the servo-control bandwidths, time-varying cross-coupling, heat dissipation, etc. However, in the final analysis, the approach was mastered to make seismic noise above 10 Hz negligible and to also control well the motion at lower frequencies, simplifying the overall controls for the interferometer.

Many resources are available for more complete descriptions of the instruments as built; this is just a snapshot of some of the features of Advanced LIGO. [18]

4.2.3 Commissioning

The Commissioning process for the ground-based interferometers involves first ensuring that the elements of the system under study are functioning, then ensuring their interfaces are correct, and then finally establishing and improving their performance to the point of usability for astrophysical searches.

During the installation process, elements are brought into service individually and then in growing subsystems to gain confidence in the functionality of the hardware, find things that need adjustment, alignment, or (hopefully) minor modifications to be suitable for the next larger step in the hierachical installation and test process. Once something of some manageable complexity has reached the point of being testable, the tests are performed and issues resolved before proceeding to a higher level of complexity.

For many of the elements of the instruments, and also for the complete detector, a next step is to bring the system into a linear regime. One example is the case of the multi-km length Fabry-Perot cavities, which only show a linear change in phase on reflection when the armlength is within about one-thousandth of an integral number of half-wavelenths of the 1 μmeter laser light – about 1 nanometer. It is also a prerequisite that the optical components be well enough aligned that most of the power is in the fundamental optical mode. We must ensure that the deviation of the beam over the 3- or 4-km arm is a fraction of the beam radius; this leads to requirements of the order of 5×10^{-5}m over 4×10^{3}m or about a micro-radian. To aid in these first goals, Advanced LIGO uses a second wavelength of light – the doubled Nd:YAG wavelength of 532 nm – to form lower-finesse cavities throughout the detector. The mirrors are specified to have lowered reflectivity for this wavelength, shortening the storage times and making the range of linear response some factor of 10-100 larger. This also provides independent measures of all of the critical lengths so that each optical cavity can be brought to resonance in a controlled and independent fashion.

Until the entire detector can be brought reliably to the linear regime (or 'locked' in the parlance of the field) the focus is on that challenge – taking it to that point, refining the process to make it more rapid, and then to make it more robust so that the locked periods are long enough to start to assess the sensitivity of the instrument. At that point, more attention can be turned to improving the performance of the system under study. As the system becomes more complete, the challenge becomes

more subtle and multi-dimensional to interpret shortcomings and develop plans of attack. One of the great results of the initial detectors was the development of individuals with the skills to contribute and also lead in this phase of the instrument preparation for astrophysical observing.

It took some 5 years in the case of Initial LIGO to go from 'installation complete' to 'ready to observe'. This was due to many factors, among them the inadequate quality control exercised, but also the fact that it was the first km-scale gravitational-wave detector to be brought into operation and the first time any of the persons involved had been through that experience. It was thus very gratifying that it took, in contrast, only a few months of commissioning for Advanced LIGO to reach a sensitivity better than that achieved with initial LIGO, and one year for the first instrument at the Livingston Observatory and only 6 months for the second at the Hanford Observatory to reach a level of stability and sensitivity that it appeared timely to start astrophysical observations.

5 The first observations

Engineering Runs are carried out between Observing runs, and immediately before them as well. As is typical, these engineering runs start a bit in advance of having all of the software and procedures in an operational mode, and in particular some of the readiness to communicate with external electromagnetic observers had not yet been reviewed and accepted. But the instruments and data analysis pipelines were ready; data distribution was established; the Detector Characterization group had established a set of vetoes to eliminate bad data; and checklists to vet detections had been drafted and iterated. On September 12, 2015, the LIGO and Virgo Collaborations declared readiness to start an Engineering run as a precursor to the start of the first 'Advanced' instrument Observing run O1, and data collection started.

5.1 GW150914

Quoting from the abstract of the publication of the first detection paper[12], "On September 14, 2015 at 09:50:45 UTC the two detectors of the Laser Interferometer Gravitational-Wave Observatory simultaneously observed a transient gravitational-wave signal. The signal sweeps upwards in frequency from 35 to 250 Hz with a peak gravitational-wave strain of 1.0×10^{-21}. It matches the waveform predicted by general relativity for the inspiral and merger of a pair of black holes and the ringdown of the resulting single black hole. The signal was observed with a matched-filter signal-to-noise ratio of 24 and a false alarm rate estimated to be less than 1 event per 203 000 years, equivalent to a significance greater than 5.1. The source lies at a luminosity distance of 410Mpc corresponding to a redshift $z = 0.09$. In the source frame, the initial black hole masses are $36M_\odot$ and $29M_\odot$, and the final black hole mass is $62M_\odot$, with $3M_\odot c^2$ radiated in gravitational waves. These observations demonstrate the existence of binary stellar-mass black hole systems. This is the first direct detection of gravitational waves and the first observation of a binary black hole merger."

The results are summarized nicely in Fig.12, taken from the paper[12]. In the upper right, one sees the signal from the Hanford Detector. The only signal processing performed is to band-pass the time series of the strain channel, removing excess

low- and high-frequency noise. The 'chirp' form of the signal is clear to the eye. In the upper right, the signals seen in the two LIGO detectors are overlapped. The Hanford signal is moved earlier in time by 7.1 msec (accounting for the fact that the signal first passed the Livingston detector and then later the Hanford detector) and inverted (because the instruments are in fact rotated 180° with respect to each other).

The middle two panels show the best-fit binary black hole waveforms, using numerical relativity results informed by analytic solutions, as well as template forms. These signals have been identically band-passed to the instrument signals, which explains the negligible signal to the left (earlier times) where in fact the strain is quasi-sinusoidal but where the signal is lost in large low-frequency noise thus removed by filtering.

The next panels show the result of subtracting the calculated best-fit General Relativity waveform from the instrument signal. Both by eye and by analysis, there is statistically no deviation of the GR result and the measurement.

The bottom two panels are spectrograms of the signal, where the chirp is visible as a rising arc in frequency-time space. This first signal took the Collaborations

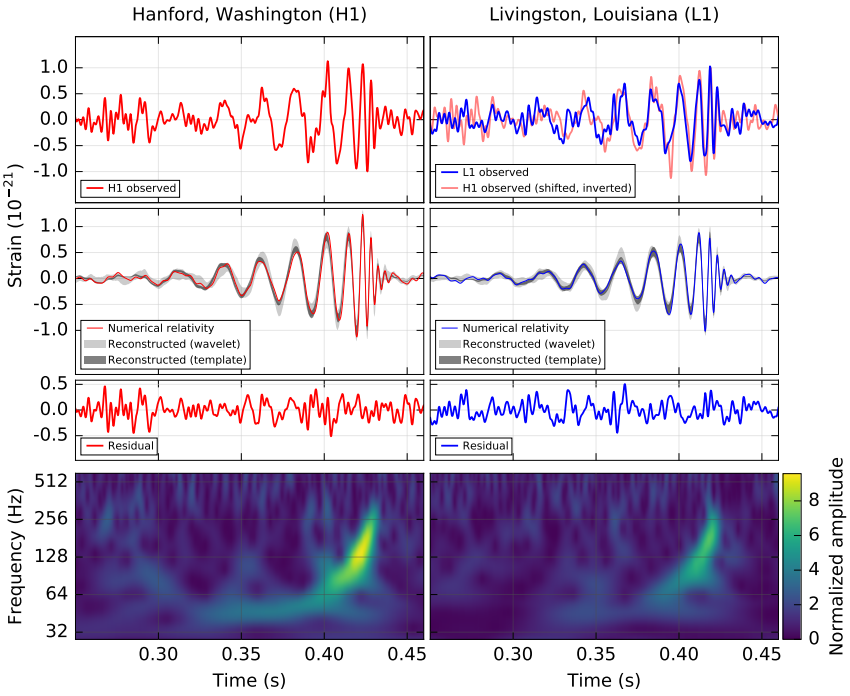

Figure 12: The first gravitational-wave signal seen by the Advanced LIGO detectors [12].

by (pleasant) surprise, and the high signal-to-noise ratio made many potentially difficult determinations much easier. The large signal size and the stationarity of the instrument background made it straightforward to calculate the probability of an accidental signal, and also rendered a detailed analysis of the signal possible. From those studies one can conclude that there are no measurable deviations in this signal from Einstein's General Relativity, and while observations of the binary pulsars continue to provide the tightest constraints on the zeroth post-Newtonian

parameter[11], many higher-order measures of agreement with the Theory could be constrained much more tightly than had been possible before.

5.2 The beginnings of gravitational-wave astrophysics and astronomy

Clearly, this first observation of the temporal variation of the amplitude of the strain in space due to gravitational waves was in itself a wonderful event, and one that yeilded rich results for general relativity and a confirmation of our understanding of the interaction of our instrument with gravitational waves. However, LIGO and Virgo were constructed with the objective of developing a new observational tool which can complement electromagnetic and neutrino observatories and this isolated signal was only a promise of what might be done.

Thus, it was a very welcome further step toward this larger future for the field that the O1 observations yeilded in total two unambiguous ($> 5\sigma$) signals, and one less significant one. All correspond to binary black holes. Figure 13[13] provides a compact graphical summary of the three signals. On the left the amplitude spectral density of the noise performance of the instruments is shown as a function of frequency. Overlaid are the trajectories in frequency and amplitude of the inspiral signals, to give a notion of the frequency range over which the signal-to-noise ratio is appreciable. On the right, the time evolution of the strain of each of the signals is shown starting from 30 Hz; this frequency is an approximation to the lowest frequency where appreciable signal can be perceived above the instrument noise. It can be seen that the signals varied in their distance, but more interestingly also in their masses. This of course shifts the frequency evolution and the maximum frequency before coalescence.

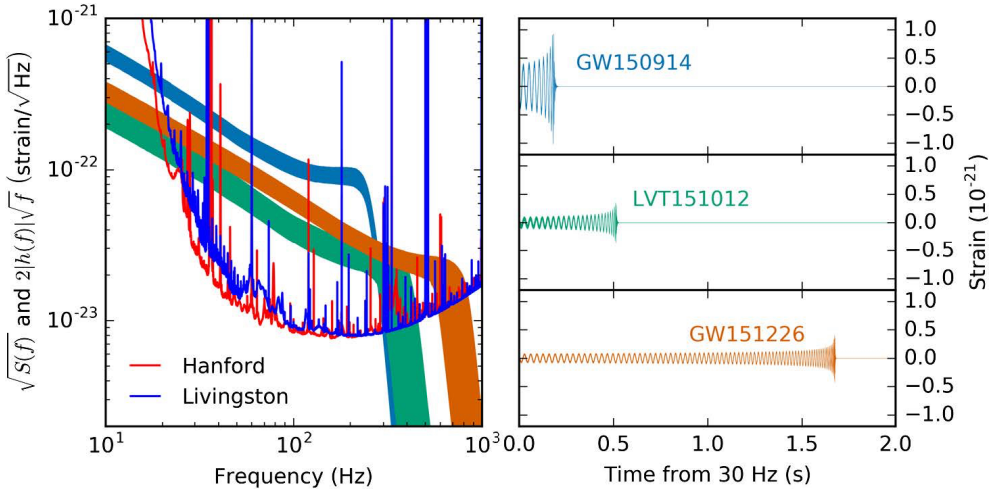

Figure 13: A graphical summary of the signals seen in the first observing run O1 for Advanced LIGO [13].

The other summary result that helps to communicate the range of information that can be abstracted from the first results[13] is found in Figure 14. Without describing all entries, it is worthwhile to draw attention to the variety of information that has been able to be inferred from these signals. Qualitatively we also see that the largest stellar-mass black holes to date are identified, that a plausible hierarchical

assembly mechanism for yet more massive black holes is seen, and that spin in the case of one of the objects is seen to be greater than zero.

Event	GW150914	GW151226	LVT151012
Signal-to-noise ratio ρ	23.7	13.0	9.7
False alarm rate FAR/yr^{-1}	$< 6.0 \times 10^{-7}$	$< 6.0 \times 10^{-7}$	0.37
p-value	7.5×10^{-8}	7.5×10^{-8}	0.045
Significance	$> 5.3\sigma$	$> 5.3\sigma$	1.7σ
Primary mass $m_1^{\rm source}/\mathrm{M}_\odot$	$36.2^{+5.2}_{-3.8}$	$14.2^{+8.3}_{-3.7}$	23^{+18}_{-6}
Secondary mass $m_2^{\rm source}/\mathrm{M}_\odot$	$29.1^{+3.7}_{-4.4}$	$7.5^{+2.3}_{-2.3}$	13^{+4}_{-5}
Chirp mass $\mathcal{M}^{\rm source}/\mathrm{M}_\odot$	$28.1^{+1.8}_{-1.5}$	$8.9^{+0.3}_{-0.3}$	$15.1^{+1.4}_{-1.1}$
Total mass $M^{\rm source}/\mathrm{M}_\odot$	$65.3^{+4.1}_{-3.4}$	$21.8^{+5.9}_{-1.7}$	37^{+13}_{-4}
Effective inspiral spin $\chi_{\rm eff}$	$-0.06^{+0.14}_{-0.14}$	$0.21^{+0.20}_{-0.10}$	$0.0^{+0.3}_{-0.2}$
Final mass $M_{\rm f}^{\rm source}/\mathrm{M}_\odot$	$62.3^{+3.7}_{-3.1}$	$20.8^{+6.1}_{-1.7}$	35^{+14}_{-4}
Final spin $a_{\rm f}$	$0.68^{+0.05}_{-0.06}$	$0.74^{+0.06}_{-0.06}$	$0.66^{+0.09}_{-0.10}$
Radiated energy $E_{\rm rad}/(\mathrm{M}_\odot c^2)$	$3.0^{+0.5}_{-0.4}$	$1.0^{+0.1}_{-0.2}$	$1.5^{+0.3}_{-0.4}$
Peak luminosity $\ell_{\rm peak}/(\mathrm{erg\,s}^{-1})$	$3.6^{+0.5}_{-0.4} \times 10^{56}$	$3.3^{+0.8}_{-1.6} \times 10^{56}$	$3.1^{+0.8}_{-1.8} \times 10^{56}$
Luminosity distance $D_{\rm L}/\mathrm{Mpc}$	420^{+150}_{-180}	440^{+180}_{-190}	1000^{+500}_{-500}
Source redshift z	$0.09^{+0.03}_{-0.04}$	$0.09^{+0.03}_{-0.04}$	$0.20^{+0.09}_{-0.09}$
Sky localization $\Delta\Omega/\mathrm{deg}^2$	230	850	1600

Figure 14: Astrophysical data gleaned from the three events seen in the first observing run O1 for Advanced LIGO [13].

Clearly, there will be much more to learn as the instruments observe for more extended periods, and as the instrument sensitivity increases through continued commissioning. The O1 run was carried out at about one-third of the Advanced LIGO design sensitivity, and ultimately we can expect a signal-to-noise ratio some three times better for these kinds of events and an event rate some $3^3 = 27$ times greater – a signal per day. The improved sensitivity will hopefully allow an unambiguous observation of the Quasi-Normal Modes of the final black hole; for GW150914, this critical phase of the signal is consistent with the QNM, but unfortunately not conclusively proof of the QNM. Beyond a larger body of data on binary black holes and more stringent tests of GR, we hope to be able to observe systems including matter (most likely neutron stars), continuous-wave sources due to eccentricity in pulsars, and of course impulsive sources which are posited to be generated by supernovæ (although current estimates for the non-spherical moment of inertia suggests that a one-per-century Milky Way Galaxy supernovæ would be required), cosmic strings, and we can also hope to have completely unexpected signals which will spark new understandings of exotic phenomena in the universe.

6 The future : ground-based Instruments

In discussing the future of ground-based gravitational-wave instruments, it becomes not only sensible but imperative to think of all detectors working as a coherent network, and so we discuss plans for both LIGO and Virgo together along with other initiatives in the world.

6.0.1 Modest improvements

The sensitivity limitations to Advanced Virgo and Advanced LIGO remain the above-discussed fundamental noise sources. We discuss each in turn, describing approaches to make modest near-term improvements to address each. The programs in this section could be realized, with adequate research and development progress as well as adequate funding, by the early- to mid-2020's.

6.0.2 Quantum Noise

Increases in the laser power to improve the (high frequency) shot-noise limit place extreme demands on many of the interferometer components. The difficulties are associated with a variety of phenomena:

- heating of optical coatings due to absorption causing changes in curvature of the optics and shifts in the resonant frequencies of the test-mass body modes
- heating of the fused-silica bulk of the test masses causing focusing of the transmitted laser beam
- torques exterted on the test masses due to finite precision and stability of the beam position with respect to the center of motion of the test masses
- impulsive momentum transfer from the photons causing length instability in the cavities
- increased light flux on the photodetectors, causing saturations in the detection chain
- potential for catastrophic 'dumping' of the stored light power, causing physical damage to optics and photodetectors

Using prepared states of light or 'squeezing' permits a 'trade' in uncertainty (while still obeying Heisenberg's dictum that $\Delta x \Delta p \geq \hbar$) which reduces the position x uncertainty in the measurement of the test mass position at high frequencies and the test mass momentum at low frequencies. This approach to precision interferometry has moved from an experimental curiosity into a practical method to improve the quantum-noise limited fringe sensitivity in an interferometer, having been demonstrated in initial LIGO and regularly used in the GEO-600 instrument. For improvements targeted in the early 2020's, frequency dependent squeezing would be employed where an optical cavity with a light storage time comparable to the multi-km arms is used to filter the squeezed light to address Δp at low frequencies where the photon pressure causes motion of the masses and to address Δx at high frequencies where the photon shot noise limits the resolution of the readout of the fringe.

6.0.3 Thermal noise

The dominant thermal noise for Advanced Virgo and LIGO is due to the mechanical losses in the multi-component dielectric layers applied to the surfaces of the test masses to create a highly-reflective optical coating. This surprising conclusion, that a thin layer some 100 μm thick and weighing a total of some 10 μg can be the

leading term, is due to the relatively large losses in these sputtered materials (some 10^{-4} loss per cycle, compared to the test mass which shows some 10^{-7} per cycle), in conjunction with the guidance from the Fluctuation-Dissipation Theorem: the place where the losses are found is where the thermal motion is the greatest. The light interacts directly with this lossy surface, and so suffers most from it.

A variety of approaches to manage this thermal noise are under study, with the most 'brute force' approach being to reduce the temperature as the motion scales with the $\sqrt{T}$; this is the approach being used by the KAGRA[14] instrument. That is not a near-term solution for LIGO and Virgo, but further research into the nature of the losses in sputtered coatings and means to reduce them incrementally are underway, and promising avenues exist for reductions by factors of 2 (so reductions in thermal noise by factors of $\sqrt{2}$ look feasible without requiring changes in the test masses or their suspensions.

6.0.4 Net performance improvements anticipated

With these improvements, reasonable models suggest that improvements in the strain sensitivity corresponding to a BNS range of $\sim$ 350 Mpc, and for BBH of 2.2 Gpc. This would lead to an increase in range of 1.6X and 1.8X respectively for BNS and $20M_{\odot}$ BBH mergers, or alternatively a detection rate increase of 6.4X (BNS) and 4.4X (BBH) with respect to Advanced LIGO or Virgo, in the early 2020's.

A further *dimension* to the observational gravitational-wave science will be the addition of the KAGRA and LIGO-India[19]. The Japanese KAGRA detector is a 3km, cryogenic, underground detector which has a planned sensitivity similar to that of Advanced Virgo and LIGO. The LIGO-India detector is an exact copy of the other two Advanced LIGO detectors, and will be placed in a 4km-arm-length infrastructure in India. It is anticipated that both of these instruments will be in full operational mode, at high sensitivity, in the early 2020's. Thus we will have 5 instruments well distributed around the globe, leading to good localization of astrophysical sources, and offering a robust system of detectors giving good duty cycle and the ability to rotate upgrades from detector to detector with minimal impact on observing. All of the Observatories plan to share data in order to extract the most science from those data.

6.1 Exploitation of the current Observatories

Looking further to the future, the goal for Virgo and LIGO will be to fully exploit the potential for gravitational-wave science in the current 3- or 4km baseline installations. One conceptual design involves a change in suspension and test mass materials (Silicon instead of fused Silica), and the use of modest cryogenics (to 123 °K), to reduce the themal noise of the suspension and coatings taking advantage of a point of the fact that the thermal expansion coefficient of Si crosses zero at that temperature. This requires a change in laser wavelength from 1 μm to 1.55 or 2 μm, and thus all optics need to be changed as well. We would also address the Newtonian background – the temporally shifting curvature of space-time around our test masses due to the compression and rarefaction of the earth stemming from seismic noise, causing the test masses to wander – with the addition of arrays of seismometers to allow this noise source to be reduced through regression. These changes could bring

another factor of 1.5 in reach and some 3-4× increase in the rate of signals, and might be realized in the mid- to late-2020's.

6.2 Concepts for new Observatories

To make a significant improvement in sensitivity over that which is possible in the current observatories will require new facilities. The concepts currently in discussion for these new Observatories take into consideration these facts:

They will have longer arms. The gravitational-wave signals in the short antenna limit grow linearly with the length of the interferometer arms, whereas the noise sources remain constant. The consequence is that the reach grows linearly with length. The lengths will be limited by practical considerations – the availability of sites, the cost and complexity of earthmoving (the sphericity of the earth is in conflict with the straight laser beams), and the cost of the vacuum and infrastructure.

They may be located underground. The seismic noise is lower underground as it distances the instrument from surface-generated noise (anthropogenic and wind) and also much seismic activity is in surface waves. It is possible to engineer solutions to reduce the direct transmission of seismic noise to the test mass, but the Newtoninan background cannot be shielded and building deep underground can move the lowest frequency perceived from the present 10 Hz to perhaps 5 or 3 Hz. KAGRA is located under a mountain, as a first experiment in this domain.

They may have a triangular configuration. This would allow both polarizations of the graviational wave to be detected at a single point, giving the cleanest information on the polarization state of the incoming gravitational wave. Additionally, sums and differences (see TDI below in connection with the space-based LISA detector) around the triangle may allow some suppression of some nuisance signals.

Cryogenics are likely to be employed, either taking advantage of specific material properties (as described in the previous section) or simply reducing thermal noise via $\sqrt{T}$.

The number of detectors will be small given the cost. A single detector of this scale might be feasible world-wide, working with the first-generation Observatories to provide localization; or the funding agencies and communities may be able to generate the enthusiasm for 2 or 3 such instruments worldwide for the richer scientific oppoortunities they will give. This will depend critically on the results from the Advanced detectors and the science advocacy undertaken to engage the greater astrophysics and astronomy communities.

Currently, two studies are underway. One is for the 'Einstein Telescope'[15] which is a European concept with significant design effort made. This calls for a triangular underground observatory with 10km arms. It would be able to house a number of parallel instruments to optimize for different frequency domains of gravitational-waves, and would be able to resolve both polarizations.

A second study in a less mature condition carries currently the name 'Cosmic Explorer'[16], and would have as its most significant feature a length of 40km. It is currently thought to be a simple 'L' shape, and effectively on the earth's surface modulo the need to make straight paths for the vacuum system and light. With such a significant length, one can imagine building an instrument with the existing Advanced LIGO or Virgo components (although larger mirrors would be needed)

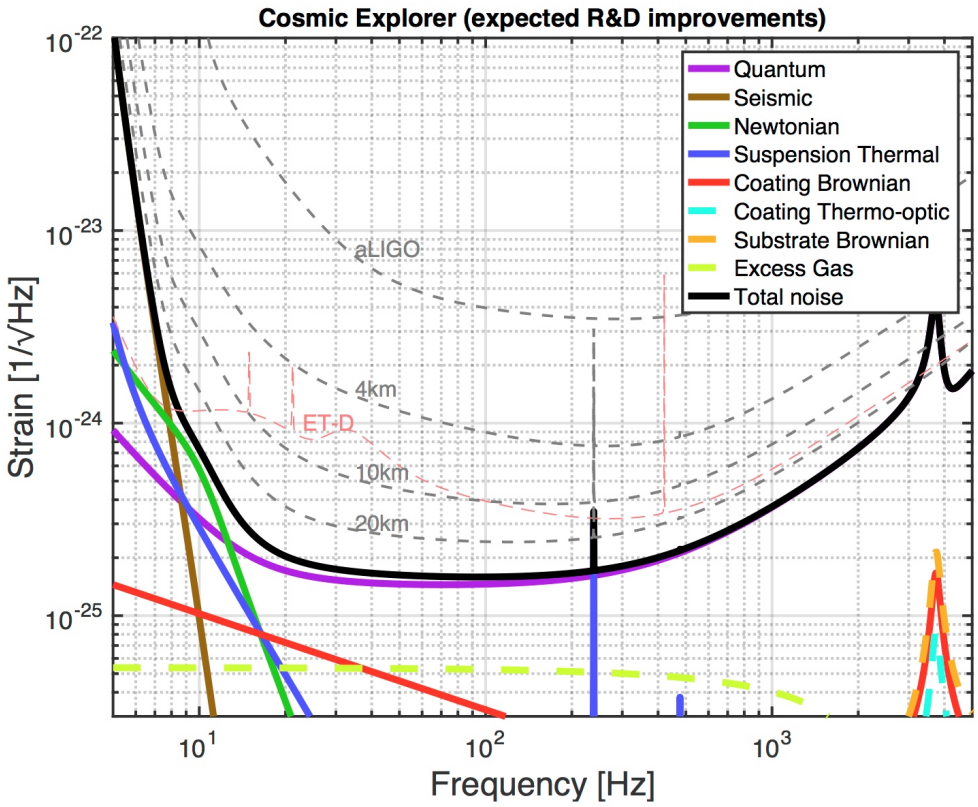

Figure 15: Possible sensitivity curves for 3rd generation Observatories and instruments [16].

and making a neat factor of 10 improvement in the sensitivity – without requiring any improvements in quantum sensing, cryogenics, thermal noise, etc. Any of these techniques could, of course, be added initially or in a second instrument installed in this infrastructure. In this sense it is a 'proof of principle' concept but nonetheless an attractive one were it to be realized.

A guess for possible sensitivities of these future Observatories and instruments is shown in Figure 15. There is a lot of optimism required to realize this future, but the technology is not likely to be the limiting factor; rather funding and a critical mass of researchers and interest in the field are the key elements.

6.3 The future : space-based Instruments

The LISA (Laser Interferometer Space Antenna) is an ESA-led project with NASA participation to put a laser-ranging gravitational-wave detector in space. It consists of a constellation of 3 spacecraft linked back and forth by six long range laser links of order 2.5 Mkm. The idea is to read the gravitational wave signals in the Doppler shifts of the coming laser light with respect to the local oscillator (see eq.12).

6.3.1 Astrophysics objectives

An interferometer in space obviously escapes all the issues of seismic noise and is superbly capable of detecting low frequency gravitational waves – $10^{-4} - 10^{-1}$ Hz. The frequency region lower than 0.1 Hz is, from an astrophysical point of view

extremely interesting. In this range are the continuous emissions of known double pulsars, allowing calibration of the instrument and maybe statistical information about this kind of stellar systems. In this range are also the transient emissions during supermassive black hole coalescences, and more generally complex phenomena around massive black holes explored by 'light' test masses in the form of stellar-mass black holes inspiraling toward a billion solar-mass black hole. This sector of research is promising for a thorough theoretical analysis of General Relativity, because high SNR can be expected, giving access to delicate details in the dynamics of such events.

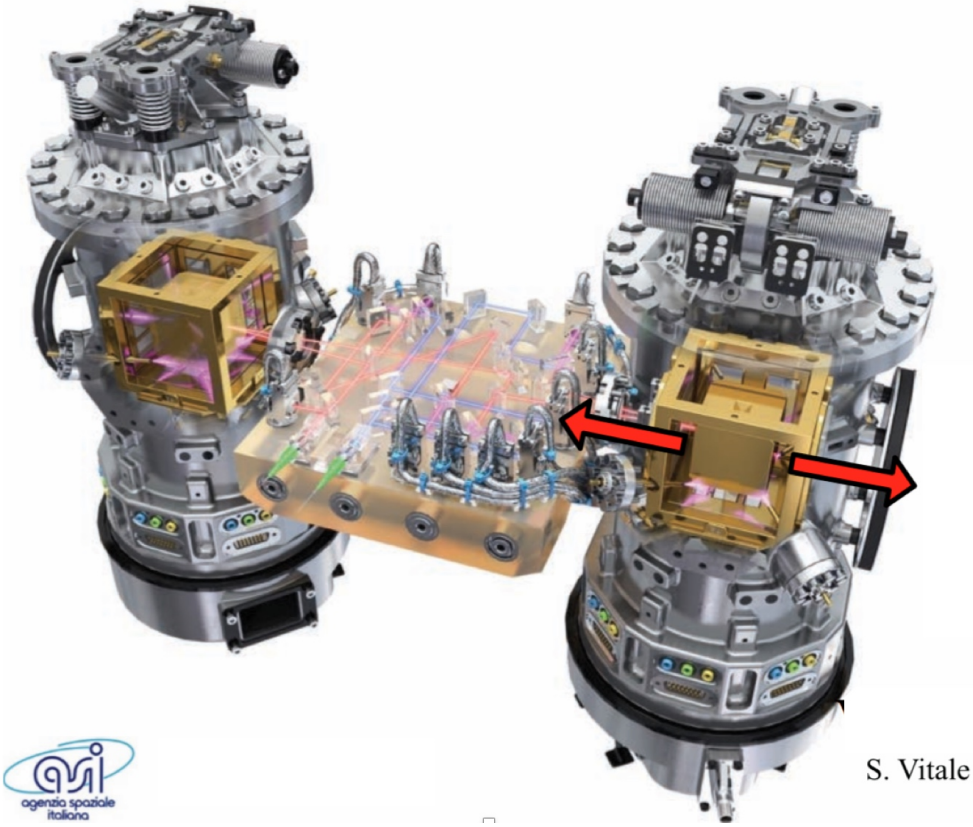

Figure 16: Drawing of the core instrument of LISA Pathfinder. *Credit: S. Vitale, U. Trento*

6.3.2 LISA Pathfinder

The very long optical path of which the small variation is to be measured through an apparent Doppler effect between two free falling test masses. This means that the test masses must not be subjected to any external perturbations, such as dust, solar wind, etc. This is possible by using a drag-free technique, i.e. protecting the test masses by an envelope (the spacecraft) and servoing the position of the envelope on the test mass by a non perturbating readout system. For "LISA", the level of isolation should be extremely high (of the order of $10^{-15}\,g/\mathrm{Hz}^{-1/2}$). This is the motivation for a technology demonstrator that has been planned by ESA since years. The mission has been recently launched toward the L1 Lagrange point (Dec. 3rd,

2015) and reported science results in March 1st, 2016. The results were excellent ([2]). This demonstration of mass shielding from external forces, control over local changes in the gravitational potential, and the interferometry needed to determine the position of the masses, has addressed most all of the technical challenges in making a space-based instrument, and the performance suffices for a full-sensitivity LISA mission. A computer-generated drawing of the core instrument of the LISA Pathfinder is shown in Fig.16. We see the two 2kg platinum-gold reference masses in their protective cages; the axis of motion is indicated by the red arrows. The interferometer formed of glass optics on a glass substrate measures the relative motion of the two masses.

6.3.3 Frequency noise reduction

Apart from the drag-free operation, many other issues are presently studied both by European and US labs. One classical issue which has been solved years ago is the question of laser noise: In real interferometers (two recombined beams interfering), the laser frequency noise can be suppressed or minimized by using symmetrical optical paths. In LISA, the beat note is between a Mkm long optical path and a 10cm one inside the spacecraft. Even with highly stabilized lasers, the noise is orders of magnitude above the faint Doppler signal. It is however possible to retrieve, by combining sampled signals of the six detected links, michelson-like structure. This way of building numerically interferometric configuration is called "TDI" (Time Delay Interferometry). One kind of algebraic structure is called "Michelson", by analogy with a real Michelson : A typical sensitivity curve is shown on Fig.17. More detailed studies have been undertaken[10]. The decrease of sensitivity at very low frequency is due to the spurious acceleration of the test masses. The decrease at high frequency is due to quantum noise.

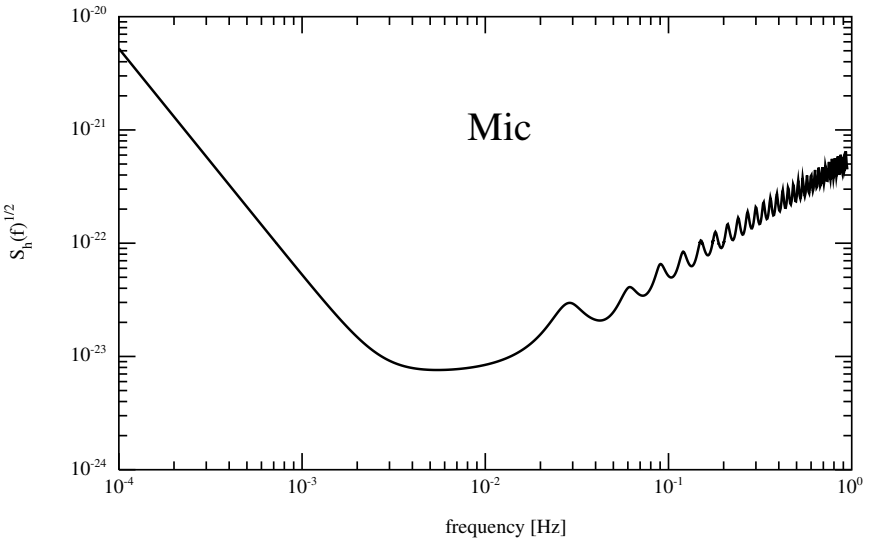

Figure 17: Sensitivity of a Michelson TDI observable for a continuous source (sky-average and one year integration).

The current timeline for LISA calls for a launch in the early 2030's. It will complement the ground-based instruments much as Radio Telescopes complement Optical Telescopes, and will be key to realizing the full potential of this new field of gravitational-wave astronomy.

References

[1] Abbott, B.P., et al.: Phys. Rev. Lett. **116**, 061102 (2016).

[2] Armano, M., et al.: Phys. Rev. Lett. **116**, 231101 (2016).

[3] Gertsenshtein, M.E., and Pustovoit, V.I.: Sov. J. Exp. Theor. Phys. **43**, 513–521 (1962).

[4] Forward, R.L.: Phys. Rev. D **17**, 379–390 (1978).

[5] Drever, R.W.P.: in : "Gravitational Radiation", edited by N. Deruelle and T. Piran, (North Holland, 1983) p.321

[6] The Virgo Physics Book
http://www.virgo-gw.eu/vpb/
or as well : http://www.bourbaphy.fr/vinet.pdf.

[7] Meers, B.J.: Phys. Rev. D **38**, 2317 (1988).

[8] Bondu, F., et al.: Phys. Rev. Lett. A **246**, 227 (1998).

[9] Weiss, R.: MIT Research Laboratory of Electronics report n.105
https://dcc.ligo.org/LIGO-P720002/public (1972).

[10] Vinet, J.-Y.: Comptes Rendus A. Sciences, Vol 14, Issue 4, Apr. 2013 pp.366–380.

[11] Burgay, M., et al.: Nature **426**, 531 (2003).

[12] Abbott, B. P., Abbott, R., Abbott, T. D., et al.: Phys. Rev. Lett. **116**, 131103 (2016).

[13] Abbott, B. P., Abbott, R., Abbott, T. D., et al.: Phys. Rev. X **6**, 041015 (2016).

[14] Aso, Y., et al.: Phys. Rev. D **88**, 043007 (2013).

[15] Abernathy, M., et al.: European Gravitational Observatory. Einstein gravitational wave Telescope: Conceptual Design Study. Technical report, 2011. http://www.et-gw.eu/etdsdocument, document number ET-0106A-10.

[16] Abbott, B. P., et al.: http://arxiv.org/abs/1607.08697.

[17] Gustafson, E., Shoemaker, D., Strain, K., Weiss, R.: LSC White Paper on Detector Research and Development, https://dcc.ligo.org/LIGO-T990080/public.

[18] Abbott, B. P., Abbott, R., Abbott, T. D., et al.: Class. Quantum Grav. **32**, 074001 (2015).

[19] Unnikrishnan, C. S.: International Journal of Modern Physics D: Gravitation, Astrophysics & Cosmology. Jan 2013, Vol. 22 Issue 1, p-1. 18p.